Proceedings Paper:

Moussa, A. and Liu, W. orcid.org/0000-0003-2968-2888 (2020) Fast and accurate range-Doppler estimation in multi-target wideband automotive FMCW radar. In: 2020 International Conference on UK-China Emerging Technologies (UCET). 2020 International Conference on UK-China Emerging Technologies (UCET), 20-21 Aug 2020, Glasgow, UK. IEEE . ISBN 9781728194899

https://doi.org/10.1109/ucet51115.2020.9205374

Fast and Accurate Range-Doppler Estimation in Multi-Target Wideband Automotive FMCW Radar

Ali Moussa and Wei Liu
Department of Electronic and Electrical Engineering
University of Sheffield, United Kingdom

***Abstract*—This paper studies the application of wideband frequency-modulated continuous-wave (FMCW) radar where the received signals are sampled first before processing. It is shown that sampling at a rate of the same order as the transmitted signal bandwidth and reducing the processed fast-time interval, helps resolve the effect of some unwanted artifacts accompanied with increasing the bandwidth and the target's radial velocity. A signal model is first developed to capture range and velocity parameters, and upper bounds are then defined on the bandwidth that separate the wideband scenario from the narrowband one; finally a novel two-stage multiple signal classification (MUSIC) based algorithm is proposed and simulation results are provided to demonstrate its performance.**

***Index Terms*—FMCW radar, MUSIC, range-Doppler.**

I. Introduction

Frequency-modulated continuous-wave (FMCW) [1] radar has been widely used in automotive applications. The transmitted signal waveform is often referred to as a chirp. Mixing a reflected chirp with the transmitted one allows extracting the range and Doppler information of a scatterer using various signal processing techniques [2], with fast Fourier transform (FFT) being the most common. Accuracy of estimation and low computational complexity have growing vitality in the automotive field as the radar is no longer limited to optional features such as parking/lane assist or adaptive cruise control; it is however an integral part of a platform that makes autonomous driving feasible [3], [4].

While increasing the bandwidth improves the range resolution of the FMCW radar, the narrowband model conventionally used degrades the accuracy of parameter estimation. In contrast, the wideband model provides a better representation of the radar signals when the bandwidth and target velocity surpass certain limits, yet it exposes several unwanted artifacts that make coherent signal processing techniques less favourable [5]. This results in the so-called range migration (RM) and Doppler frequency migration (DFM) problems in range-Doppler processing [6].

For digital processing of radar signals, it is usually desirable to have lower sampling rates to reduce cost and complexity. This is easily achieved in conventional automotive FMCW radar when the received signal is first mixed with the transmitted signal resulting in a relatively low bandwidth deramped signal suitable for low sampling rates. However, the race towards the digital radar and the capacity of high sampling rates and large memory motivate the idea of moving the sampling stage closer to the receiver antenna. It will be shown in this work that high sampling rates (the same order as the transmitted signal bandwidth) not only increase the maximum unambiguous range, but also allow processing a very small portion of the sampled chirp duration, which can then resolve the effect of some artifacts while relaxing the duration of the analogue transmitted chirp.

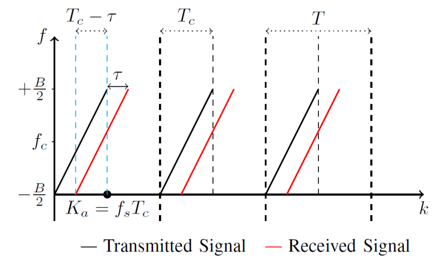

Fig. 1. A set of transmitted and received FMCW signals represented as frequencies against sampled time.

In this paper, a detailed wideband signal model is presented first for automotive FMCW radars. We analyse terms that are often discarded in existing literature. After that, upper bounds are defined on the signal bandwidth that separates the narrowband model from the wideband one. Using these bounds, an oversampling scheme is proposed that allows resolving the effect of the unwanted artifacts of wideband FMCW radar. Then, in order to reduce the computational complexity of a traditional two dimensional (2D) search, a novel two-stage algorithm for parameter estimation is developed based on the classic 1D-MUSIC algorithm [7]. By decoupling the range and Doppler domains using two 1D searches, pairing the estimated parameters becomes a major drawback. To overcome this issue, the Clean technique proposed in [8] is employed to pair the estimated parameters of multiple targets in a precise novel manner. Finally, some simulation results are provided to validate the proposed ideas.

II. Signal Model

A. Wideband FMCW Signal Model

Consider a FMCW transceiver in operation where there exist I moving targets in the far-field with unknown parameter vector $\mathbf{\Phi}_i = [R_i, v_i]$. The aim is to estimate the range R and the radial velocity v. The radar transmits FMCW chirp signals with a chirp length T_c, centre frequency f_c and bandwidth B as shown in Fig. 1. Every M transmitted chirps constitute a frame of length MT, where T is the chirp repetition interval. The time t can be decomposed into fast-time and slow-time domains referred to as t_f and m respectively, and can therefore be modelled as

$$t_{m,t_f} = t_f + mT \quad t_f \in [0, T_c), \tag{1}$$

where $m = [0, 1, \cdots, M-1]$. The transmitted chirp is periodic and can be written in the complex form as

$$s(t_f) = e^{j2\pi(f_c t_f + 0.5\mu t_f^2)}, \tag{2}$$

where $\mu = \frac{B}{Tc}$ is the chirp rate.

A moving scatterer i in the observation field of the radar causes a round trip time delay to the inital transmitted signal. This time delay can be modelled as

$$\tau_i(m, t_f) = \frac{2R_i}{c} + \frac{2v_i}{c}(t_f + mT), \tag{3}$$

where c is the speed of light. The reflected signal from the ith target can be modelled as

$$r_i(m, t_f) = \alpha_i s(t_f - \tau_i(m, t_f)) = \alpha_i e^{j\phi_i(m,t_f)}, \tag{4}$$

where α_i is the complex amplitude of the ith scatterer. After expanding, $\phi_i(m, t_f)$ can be written as

$$\begin{aligned}\phi_i(m, t_f) = [&f_c((1 - \frac{2v_i}{c})t_f - \frac{2v_i}{c}mT - \frac{2R_i}{c}) \\ &+ 0.5\mu((1 - \frac{2v_i}{c})t_f - \frac{2v_i}{c}mT - \frac{2R_i}{c})^2].\end{aligned} \tag{5}$$

The period of active transmission T_c is then sampled at a rate f_s resulting in discrete-time transmitted and received signals. In Fig. 1, K_a respresents the available fast-time samples for the chirp duration T_c. In order to extract the unknown range and velocity, we cross-correlate the transmitted and the received signals. The resulting deramped signal for the ith scatterer can be written in the discrete-time format as

$$\begin{aligned}&r_i(m, k)s^*(k) \\ &= \alpha_i \exp[-j2\pi(\frac{2f_c R_i}{c} - \frac{2\mu R_i^2}{c^2} + (f_{d,i} - \frac{4\mu R_i v_i}{c^2})mT \\ &+ (f_{r,i} + f_{d,i} - \frac{4\mu R_i v_i}{c^2})\frac{k}{f_s} + (\frac{2\mu v_i}{c} - \frac{4\mu v_i^2}{c^2})\frac{k}{f_s}mT \\ &+ (\frac{2\mu v_i}{c} - \frac{2\mu v_i^2}{c^2})\frac{k^2}{f_s^2} - \frac{2\mu v_i^2}{c^2}m^2T^2)],\end{aligned} \tag{6}$$

where $f_{d,i} = \frac{2f_c v_i}{c}$, $f_{r,i} = \frac{2\mu R_i}{c}$, $k = [0, 1, \cdots, K-1]$ and K is the total number of fast-time samples.

Due to the automotive application being modelled, the order of v_i and R_i is much smaller than that of the speed of light c, so all terms in (6) that contain c^2 can be discarded. Moreover, $(\frac{2\mu v_i}{c} - \frac{2\mu v_i^2}{c^2})\frac{k^2}{f_s^2}$ is a second-order fast-time term. It is negligible when the range resolution is in the order of centimeters or above, so it can also be discarded.

The simplified discrete-time deramped signal can now be written as

$$\begin{aligned}y_i(m, k) = \hat{\alpha}_i \exp\Bigg[- j2\pi\Bigg(&f_{d,i}mT + (f_{r,i} + f_{d,i})\frac{k}{f_s} \\ &+ \frac{2\mu v_i}{c}\frac{k}{f_s}mT\Bigg)\Bigg],\end{aligned} \tag{7}$$

where $\hat{\alpha}_i$ contains the dimensionless constant term $\frac{2f_c R_i}{c}$.

B. Modelling of Unambiguous Regions and Resolution Bounds

Taking into account the Nyquist considerations, the maximum unambiguous regions for velocity and range can be modelled respectively as

$$v_m = \frac{c}{4Tf_c}, \quad R_m = \frac{cf_s}{2\mu}. \tag{8}$$

The resolution bounds can be estimated using the Rayleigh criterion. The velocity resolution bound can be defined as

$$v_{\text{res,max}} = \frac{c}{2f_c MT}. \tag{9}$$

Assuming the observation period in the fast-time domain is equal to the chirp duration, the range resolution bound can then be defined as

$$R_{\text{res,max}} = \frac{c}{2B} - \frac{2v_m f_c}{\mu}. \tag{10}$$

III. Analysis of Unwanted Artifacts

A. Coupling Term

The term $\frac{2\mu v_i}{c}\frac{k}{f_s}mT$ in (7) couples the fast-time domain with the slow-time domain and degrades the orthogonality between these domains. It is responsible for RM and DFM in range-Doppler processing. In the following, the severity of the coupling term is first quantified. Accordingly, bandwidth bounds that separate the narrowband model from the wideband one are defined. The analysis is done for range and velocity respectively.

When a range search is done across the fast-time domain, the first order terms along with the coupling term can be written as $[(f_{r,i} + f_{d,i} + \frac{2\mu v_i}{c}mT)\frac{k}{f_s}]$. The maximum bias in range due to coupling can be quantified as

$$R_{\text{bias,max}} = v_m(M-1)T. \tag{11}$$

This bias becomes severe once it is larger than the resolution of the range search. Consequently, RM degrades the accuracy of range estimation. So, in order to avoid RM, the following condition needs to be satisfied

$$R_{\text{bias,max}} < R_{\text{res,max}}. \tag{12}$$

Using (8), (10), (11) and (12), we define the following upper bound on bandwidth below which RM has negligible effect on range estimation

$$\beta_r = \frac{2f_c}{(M-1)}\left(1 - \frac{T_c}{T}\right). \tag{13}$$

When a velocity search is done across the slow-time domain, the first order term along with the coupling term can be written as $[(f_{d,i} + \frac{2\mu v_i}{c}\frac{k}{f_s}mT]$. The maximum bias in velocity due to coupling can be quantified as

$$v_{\text{bias,max}} = \frac{B(K_p - 1)v_m}{T_c f_c f_s}. \tag{14}$$

Similar to RM, the velocity bias causes DFM which can be avoided should the bandwidth adhere to an upper bound of

$$\beta_v = \frac{2f_c T_c f_s}{M(K_p - 1)}, \tag{15}$$

where K_p is total number of processed fast-time samples.

Note that the defined upper bounds on bandwidth are based on the Rayleigh criterion which underestimates the super-resolution capability of some advanced parameter estimation techniques. So, we propose making the bounds stricter by certain folds depending on the super-resolution capability of the technique used.

B. Steering Vector with Multiple Parameters

In an ideal parameter estimation scenario, the fast-time and slow-time domains only contain range and Doppler information respectively. However, while ignoring the coupling term in (7), we can observe that in a wideband FMCW scenario, the fast-time domain contains both Doppler and range information. Unlike coupling, this artifact introduces a constant shift in energy rather than a smearing-like effect. Here, we define the parameter(s) steering vectors corresponding to the slow-time and fast-time domains respectively: Although the slow-time domain is free of this artifact, its steering vector is defined for the sake of completion as

$$\mathbf{v}_i = [1, e^{-j2\pi f_{d,i}T}, \cdots, e^{-j2\pi f_{d,i}(M-1)}]^T, \tag{16}$$

where $\{.\}^T$ is the transpose operator.

In the fast-time domain, the steering vector can be defined as

$$\mathbf{r}_i = [1, e^{-j2\pi\frac{(f_{r,i}+f_{d,i})}{f_s}}, \cdots, e^{-j2\pi\frac{(f_{r,i}+f_{d,i})}{f_s}(K-1)}]^T. \tag{17}$$

IV. The Proposed Two Stage 1D-MUSIC based Algorithm

A. Resolving the Artifacts

By first ignoring the coupling effect, we propose solving the artifact of multiple parameters in the fast-time domain using a two-stage parameter estimation method based on the classic 1D-MUSIC. As the slow-time contains Doppler information only, we first search the slow-time domain for the velocity parameters within the unambiguous region. After that, we confine the velocity region to the estimated velocity parameters, and search the fast-time domain for the range parameters within the unambiguous region.

This proposed method allows estimating each parameter accurately without an exhausting 2D search. Along with our proposed sampling scheme, it also facilitates resolving the coupling problem. In the first stage of the algorithm, K_p is chosen so that it satisfies the bandwidth bound in (15). The velocity parameters can then be accurately estimated without suffering from DFM. One can argue that processing K_p fast-time samples such that $K_p \ll K_a$ reduces the integration gain in Doppler processing. However, the increasing bandwidth in a wideband scenario and the larger unambiguous range reduces the correlation between the fast-time samples which compensates for the reduction in signal-to-noise ratio (SNR).

In the second stage, for each estimated velocity, the coupling term causing RM can be filtered out from the raw data before searching for the corresponding range parameter. Another argument here stems from the fact that the information bandwidth may be much lower than the sampling rate in a typical automotive scenario. So, we propose decimating the raw data before range processing which reduces the number of available fast-time samples. The decimation factor D can be defined as

$$D = \frac{f_b}{f_s}, \tag{18}$$

where $f_b \approx \frac{2\mu R_m}{c}$ is the information bandwidth.

In a multiple targets case, even though the doppler information is known, filtering the coupling terms corresponding to all targets simultaneously before the second stage can add extra range bias to some targets and degrade the performance of the range search. Also, implementing a 1D search for range estimation makes it difficult to pair the estimated targets' range with the correct velocity. Here it is proven that filtering out the coupling terms individually not only removes their effect, but also allows pairing the peaks in the range-MUSIC spectrum with the correct corresponding velocities.

Consider a noiseless case of two targets with ranges and velocities (R_1, R_2) and (v_1, v_2) respectively. Assume the velocities are accurately estimated as $(\check{v}_1, \check{v}_2)$, and the targets have the same intensity. After filtering out the coupling due to $\check{v}_1$, the k-th fast-time term of the resulting deramped signal can be written as

$$e^{-j2\pi(f_{r,1}+\frac{2\mu(v_1-\check{v}_1)}{c}mT)\frac{k}{f_s}} + e^{-j2\pi(f_{r,2}+\frac{2\mu(v_2-\check{v}_1)}{c}mT)\frac{k}{f_s}} \tag{19}$$

Since $v_1 = \check{v}_1$, target 1 now has maximum integration gain (maximum orthogonality between its search vector and the noise space in noisy subspace-based processing) and its correponding peak in the range-MUSIC pseudo-spectrum is maximised and is larger than of target 2. The right hand side term in (19) *still suffers from coupling because $v_2 \neq \check{v}_1$. Similarly, when coupling due to $\check{v}_2$ is filtered out, the peak in the range-MUSIC pseudo-spectrum corresponding to target 2 is maximised and is larger than that of target 1.*

In the case of multiple targets with different intensities, the Clean technique is utilised where targets are sorted in the descending order of intensities before processing. After estimating the range of each in the defined order, the target profile is reconstructed and removed from the raw data.

B. Reshaping the Raw Data

The raw data represented in the signal model (7) is stored and reshaped into a matrix format as $\mathbf{Y} \in \mathbb{C}^{M\times K}$ such that

$$\mathbf{Y} = \sum_{i=1}^{I} \hat{\alpha}_i \mathbf{v}_i \mathbf{r}_i^T \odot \mathbf{C}_{\mathbf{v}i} + \mathbf{N}, \tag{20}$$

where $\{\odot\}$ is the Hadamard product. $\mathbf{C}_{\mathbf{v}i}$ is a $M \times K$ matrix whose k-th column is given by

$$\mathbf{p}_{\mathbf{v}i}(k) = [1, e^{-j\frac{4\pi\mu v_i}{c}\frac{kT}{f_s}}, \cdots, e^{-j\frac{4\pi\mu v_i}{c}\frac{k(M-1)T}{f_s}}]^T. \tag{21}$$

$\mathbf{N} \in \mathbb{C}^{M\times K}$ is the additive white Gaussian noise of zero mean and variance σ^2.

C. Two-Stage 1D-MUSIC Based Algorithm

First, the reshaped data matrix $\mathbf{Y}$ is constructed such that $K = K_p$ satisfies the bound in (15). $\mathbf{Y}$ is then used to perform a velocity search using 1D-MUSIC. The velocity steering vector spans the entire unambiguous region $[-v_m, v_m]$. The estimated velocities $[\check{v}_1, \ldots, \check{v}_I]$ are sorted in the descending order of intensity and stored to be implemented in the second stage.

Then, following the sorted order of intensities, for each $\check{v}_i$, $\mathbf{C}^*_{\check{\mathbf{v}}i}$ and $\mathbf{Y}^T$ are constructed such that $K = K_a$, where $\{.\}^*$ denotes the complex conjugate. The coupling term causing RM is then filtered out and the new reshaped data matrix can be written as

$$\mathbf{Y'}^T = (\mathbf{Y} \odot \mathbf{C}^*_{\check{\mathbf{v}}i})^T \tag{22}$$

$\mathbf{Y'}^T$ is then multiplied by a decimation matrix $\mathbf{D} \in \mathbb{R}^{DK_a \times M}$ which constitutes of the Dkth rows of the identity matrix $\mathbf{I} \in \mathbb{R}^{K_a \times K_a}$. After that, a range search is performed using 1D-MUSIC where the range steering vector spans the entire unambiguous region $[0, R_m]$. The largest peak in the range-MUSIC pseudo-spectrum corresponds to the estimated range $\check{R}_i$. The estimated range and velocity parameters $(\check{R}_i, \check{v}_i)$ are used to construct the target profile which is then subtracted from the raw data matrix before processing the next target.

V. Simulation Results

TABLE I
Radar Parameters

Parameter	Value	Parameter	Value
f_c	77 GHz	B	$1 - 5$ GHz
T_c	50 μs	T	100 μs
f_s	1 Gsps	K_a	$50,000$
K_p	512	M	128

TABLE II
Target Parameters

Target	Intensity (dB)	Range (m)	Velocity (m/s)
1	-1	4.789	-7.407
2	-2	34.547	7.084
3	-3	30.923	5.319
4	-4	11.443	-4.167
5	-5	25.390	2.625

Monte-Carlo computer simulations are performed in order to test the ability of the proposed algorithm in accurately estimating the motion parameters of multiple targets without suffering from the unwanted artifacts of the wideband FMCW scenario. The root-mean-square error (RMSE) of each motion parameter for the proposed method is compared to that of a conventional FMCW approach, where the range-Doppler processing is done as in [9] under narrowband assumptions. Five targets are placed in the visible region of the radar and their parameters are shown in Table II. The used radar parameters are shown in Table I.

From Fig. 2(a), it can be observed that velocity RMSE of the proposed method is significantly low compared to that of a conventional narrowband-based method. It stays flat as the bandwidth increases because the latter does not exceed the bound in (15), while for the conventional method it increases with the bandwidth as theoretically expected. From Fig. 2(b), the proposed method at low SNR yields much higher error

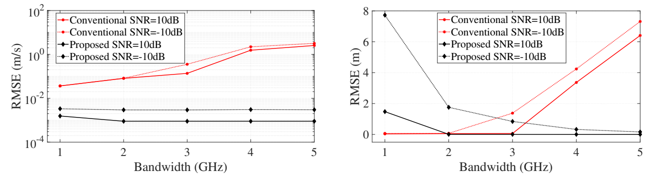

(a) velocity estimation (b) range estimation

Fig. 2. Comparison of RMSEs between the proposed and the conventional methods as a function of bandwidth.

than the conventional one at low bandwidth. This is due to mismatch in the pairing process. However, as the bandwidth increases, the performance of range estimation improves largely using the proposed method which outperforms the conventional one above 3 GHz. This conveys the potential of the proposed two-stage processing for ultra-wideband FMCW radar.

VI. Conclusion

A model for wideband FMCW radar has been presented, which unfolds several unwanted artifacts that degrade the performance of range-Doppler estimation using conventional methods. These artifacts were explicitly analysed and upper bounds were defined on modulation bandwidth that separates the wideband model from the narrowband one. By implementing the bandwidth bounds, an oversampling scheme was proposed that allows processing a very short fast-time period in the Doppler domain and consequently resolves the effect of RM, followed by a novel two-stage algorithm for range-Doppler processing for decoupled domains. As shown by computer simulations, a much better performance has been achieved by the proposed approach.

References

[1] A. G. Stove, "Linear fmcw radar techniques," *IEE Proceedings F - Radar and Signal Processing*, vol. 139, no. 5, pp. 343–350, 1992.

[2] S. M. Patole, M. Torlak, D. Wang, and M. Ali, "Automotive radars: A review of signal processing techniques," *IEEE Signal Processing Magazine*, vol. 34, no. 2, pp. 22–35, 2017.

[3] F. Engels, P. Heidenreich, A. M. Zoubir, F. K. Jondral, and M. Wintermantel, "Advances in automotive radar: A framework on computationally efficient high-resolution frequency estimation," *IEEE Signal Processing Magazine*, vol. 34, no. 2, pp. 36–46, 2017.

[4] I. Bilik, O. Longman, S. Villeval, and J. Tabrikian, "The rise of radar for autonomous vehicles: Signal processing solutions and future research directions," *IEEE Signal Processing Magazine*, vol. 36, no. 5, pp. 20–31, 2019.

[5] G. Hakobyan and B. Yang, "High-performance automotive radar: A review of signal processing algorithms and modulation schemes," *IEEE Signal Processing Magazine*, vol. 36, no. 5, pp. 32–44, 2019.

[6] W. Cui, S. Wu, Q. Shen, J. Tian, S. Wu, and X. Xia, "Parameter estimation method for radar maneuvering target with arbitrary migrations," *IEEE Transactions on Aerospace and Electronic Systems*, vol. 55, no. 5, pp. 2195–2213, 2019.

[7] R. Schmidt, "Multiple emitter location and signal parameter estimation," *IEEE Transactions on Antennas and Propagation*, vol. 34, pp. 276–280, March 1986.

[8] J. Tsao and B. D. Steinberg, "Reduction of sidelobe and speckle artifacts in microwave imaging: the clean technique," *IEEE Transactions on Antennas and Propagation*, vol. 36, no. 4, pp. 543–556, 1988.

[9] J. W. Odendaal, E. Barnard, and C. W. I. Pistorius, "Two-dimensional superresolution radar imaging using the music algorithm," *IEEE Transactions on Antennas and Propagation*, vol. 42, no. 10, pp. 1386–1391, 1994.